ELSEVIER

Journal of Alloys and Compounds 446–447 (2007) 58–62

Journal of ALLOYS AND COMPOUNDS

www.elsevier.com/locate/jallcom

Catalytic properties on the hydrogen desorption process of metallic additives dispersed in the MgH_2 matrix

R. Checchetto[a,*], N. Bazzanella[a], A. Miotello[a], P. Mengucci[b]

[a] *Dipartimento di Fisica dell'Università di Trento, Via Sommarive 14, I-38050 Povo (TN), Italy*
[b] *Dipartimento di Fisica ed Ingegneria dei Materiali e Territorio, Università Politecnica delle Marche, I-60131 Ancona, Italy*

Received 13 September 2006; received in revised form 2 November 2006; accepted 7 November 2006
Available online 8 December 2006

Abstract

Composite transition metal (TM)-doped magnesium samples (TM = Nb, Fe and Zr) were produced by r.f. magnetron sputtering. The hydrogen desorption kinetics of the TM-doped MgH_2 samples was studied by Sievert analysis and its thermal stability by thermal desorption spectroscopy (TDS). Energy dispersive spectroscopy (EDS) analysis indicates that the additive is contained in the magnesium bulk at 10^{-2} atomic concentration. The microstructural characterization of the sample was carried out by X-rays diffraction spectroscopy (XRD) and the obtained spectra indicate that, in the activated MgH_2 samples, the TM additive is contained in form of nanosized clusters. TDS spectra and isothermal H_2 desorption curves indicate that the TM nanoclusters dispersed in the MgH_2 matrix reduce its thermal stability and accelerate the H_2 desorption kinetics as compared to the pure MgH_2 samples. The improved H_2 desorption properties can be explained by the presence of extended interfaces between MgH_2 and TM nanoclusters acting as heterogeneous nucleation sites, with reduced activation energy, for the h-Mg phase and fast diffusion channels for H migrating atoms.

Keywords: Metal hydride; Catalyst; X-rays diffraction; Thermal analysis

1. Introduction

Due to the high hydrogen storage capacity of MgH_2, ~7.6 wt.%, the low cost and weight, magnesium is an important candidate for H_2 storage applications. Most research efforts are dedicated to the catalysis of the H_2 sorption processes that is too slow even at temperatures larger than 500 K because: (i) the usual presence of a surface oxide Mg layer [1], (ii) the poor ability of the oxidized and pure Mg surface to dissociate H_2 molecules [2] and (iii) the formation of a continuous MgH_2 layer at the Mg surface during hydrogenation acting as hydrogen diffusion barrier [3]. The hydrogen absorption and desorption kinetic in Mg can be significantly improved by microstructural refinements as well as with the nanocrystalline structure of the Mg particles because grain boundaries are: (i) active sites for the nucleation processes in the metal to hydride (or reverse) phase transition and (ii) preferential diffusion paths for H atoms [4].

Mixing Mg or MgH_2 powders with transition metals or metal oxides gives rise to a further improvement of the H_2 sorption kinetics. Liang et al. [5] have shown that the composite material formed by milling MgH_2 and V powders (5 at.% concentration) completely desorbs H_2 in 200 s at 573 K while about 2000 s are required by milled MgH_2. XRD analysis showed the formation, during the H_2 absorption process, of the MgH_2 and VH_x ($x < 0.81$) phases and the authors suggested that the V catalyst favours the dissociation of the H_2 molecule and the transfer of H atoms to the nanocrystalline Mg layers by a mechanism involving the H atomic migration through the catalyst. The microscopic mechanism leading to the catalytic effect is under debate. To analyse whether the transport of the reactive H atoms to the Mg layers is related to the H diffusion through the catalyst layers ("hydrogen pump") or to the catalyst surface ("spill-over"), Pelletier et al. carried out in situ time resolved synchrotron measurement during H_2 desorption of the $MgH_2 + 5$ at.% Nb composite material at 583 K; during the H_2 desorption process the authors observed the transformation of the catalyst nanocluster from the β-NbH phase to the metastable ε-NbH_x phase [6]. The catalytic effect of Nb was thus explained as consisting on the fast hydrogen transport through the ε-NbH nanoclusters where

---

[*] Corresponding author. Tel.: +39 0461 881650; fax: +39 0461 881696.
E-mail address: checchet@science.unitn.it (R. Checchetto).

0925-8388/$ – see front matter © 2006 Elsevier B.V. All rights reserved.
doi:10.1016/j.jallcom.2006.11.017

the interstitial migration of hydrogen atoms is a fast process due to the large interatomic distances in the ε-NbH_x unit cell. The existence of the ε-NbH phase at temperatures ~600 K is difficult to explain because it is stable under 204 K and its role in the catalytic process was questioned by Yavari et al. [7]; using a high brilliance X-rays beam for diffraction analysis of MgH_2 + 5 at.% Nb composites during H_2 desorption above 573 K, the authors observed the formation of a supersaturated Nb–H solid solution and thus excluded the formation of the ε phase. They suggested that H atoms dissociated at the Nb surface are attracted to the Nb/Mg interface because the formation of Mg–H and Nb–H bonds reduces the high Nb–Mg interfacial energy and that the accelerated H_2 sorption kinetics can be explained by the fast H diffusion kinetics along such extended defects.

We have recently studied the H_2 desorption process from MgH_2 samples where the metallic additive was completely included in the MgH_2 matrix [8,9]. Microcrystalline Nb-doped Mg samples grown by co-sputtering Nb and Mg targets showed an improved H_2 desorption kinetics as compared to that of pure Mg; the time required for 50% MgH_2 transformation at 623 K, for example, was reduced from ~3200 to ~110 s in MgH_2 samples containing 5 at.% Nb. While in MgH_2 samples, the H_2 desorption kinetics was controlled by the nucleation and growth of the h-Mg phase with activation energy of 141 kJ/mol, the desorption process in Nb-doped samples showed an activation energy value of 51 kJ/mol, close to that of the H atomic diffusion through transformed h-Mg layers. Structural analysis by EXAFS and TEM proved that the catalytic activity of Nb doping was connected with Nb clustering producing, in the hydrogenated material, Nb:H nanoclusters dispersed in the MgH_2 matrix [10]. It was suggested that Nb doping accelerates the hydrogen desorption by the presence of extended interfaces between MgH_2 and additive nanoclusters which act as heterogeneous sites for h-Mg nucleation and fast diffusion channels for H migrating atoms.

In this paper, we present a comparative study on the H_2 desorption from the MgH_2 matrix doped with different metallic elements dispersed in atomic concentration, 2–5%; we have chosen Fe, Nb and Zr because: (i) they are transition metals (TM) with catalytic properties for the H_2 sorption kinetics in Mg, (ii) they do not form binary phases with Mg and show negligible solubility [11] and (iii) they allow a comparison between elements that in the examined temperature range ($400\ K < T < 700\ K$): (1) forms interstitial alloys with hydrogen (Nb: α phase that is a random interstitial alloy of H in bcc Nb, for $X_H < 0.31$), (2) forms stable phase (Zr: δ phase having fcc structure with $1.31 < X_H < 2$) and (3) Fe, that does not form any binary hydride phase and shows negligible H solubility [12].

2. Experimental details

Mg and metal-doped Mg samples (metal = Nb, Fe and Zr) were deposited in form of thick films (thickness of 10–20 μm) on graphite wafers (g-C) by r.f. magnetron sputtering using 99.97% purity Ar as working gas and 99.95% purity Mg as target material. The background pressure in the chamber was in the low 10^{-5} Pa order; the deposition process was carried out at 0.5 Pa Ar pressure and 150 W r.f. power without substrate heating. The metal doping of the Mg films was obtained by inserting small TM fragments (squares with ~3 mm side) over that part of the Mg target which is preferentially eroded and the metal content was controlled after deposition by EDS technique. To prevent surface oxidation and stimulate the H_2 dissociation, the pure Mg and the TM-doped Mg samples were coated with a ~20 nm thick Pd capping layer by rotating the sample holder over a 99.9 at.% purity Pd target without interrupting the vacuum conditions. The film samples deposited on g-C peeled off from the substrates after exposure to air at ambient conditions. The self-supporting samples were thus introduced in a Sievert-type apparatus for H_2 cycling and the study of the isothermal sorption kinetics [13]. The activation procedure of the samples consisted on repeated absorption and desorption cycles at 623 K and 1.0 or 0.015 MPa H_2 (or D_2) pressure for absorption and desorption, respectively. The activated samples are then exposed at temperatures between 583 and 623 K to H_2 (or D_2) gas at 1.2 MPa and vacuum for H_2 absorption and desorption, respectively. The structural and kinetic analysis presented in this paper refer to completely activated samples; upon H_2 cycling the activation was considered as complete when the H_2 absorption and desorption curves resulted repeatable upon further cycling. The structural characterization of the pure and metal-doped Mg film samples was carried out by X-rays diffraction spectroscopy (XRD) in Bragg–Brentano (θ–2θ) configuration at 40 kV and 40 mA using the Cu Kα radiation. The thermal stability of pure and TM-doped MgD_2 samples were studied by TDS analysis. Measurements were carried out by heating the sample in a UHV chamber with a linear temperature ramp of ~0.16 K/s and recording the D_2^+ mass signal ($m/e = 4$) of a quadrupole mass spectrometer equipped with secondary electron multiplayer at constant pumping speed of the pumping apparatus [14]; for the TDS analysis deuterium was chosen rather than hydrogen to improve the signal-to-noise ratio; at 2% of the TDS peak height the signal-to-noise ratio of the $m/e = 4$ signal was better than 10^2.

3. Results and discussion

EDS analyses on the metal additive content in the Mg samples show doping in the at.% level: ~5 at.% for Fe and Nb and ~3 at.% for Zr; these concentrations are larger than the maximum solubility of the TM in Mg, 0.00043 at.% for Fe at the eutectoid temperature of 920 K, close to 1.3×10^{-4} for Nb in liquid Mg at 1500 K, and lower than 0.1 at.% for Zr at temperatures lower than 700 K [11]. These equilibrium properties indicate that precipitation of the metal additive atoms is expected upon the thermal treatment leading to the sample activation at 623 K and/or during H_2 cycling. The room temperature XRD spectra of the TM-doped samples, partially de-hydrogenated, confirm cluster formation, see Fig. 1. It can be observed that the Mg layers in all the TM-doped samples maintain the preferential (0 0 2) orientation as in the as-deposited sample [8]. This preferential orientation of the Mg layers does not change also after repeated absorption and desorption cycles. While Fe remains in the metallic state, Nb and Zr form hydride phase as shown by the $NbH_{0.89}$ and $ZrH_{1.66}$ reflection peaks; no evidence of metallic Nb or Zr was found in the hydrogenated samples. The obtained TM–H phases are appropriate to equilibrium phase diagram at room temperature [12]. The Debye–Scherrer analysis of the XRD peak indicates the formation of TM nanoclusters having dimensions in the 10–20 nm range, while Mg and MgH_2 maintain a microcrystalline structure [8,9].

In Fig. 2, we present the isothermal H_2 desorption curves of the pure and metal-doped MgH_2 samples at the representative temperature of 623 K. The curves show a strong improvement of the H_2 desorption kinetics in the examined TM-doped samples when compared to the pure MgH_2; at this temperature the interval time required for 50% transformation decreases from

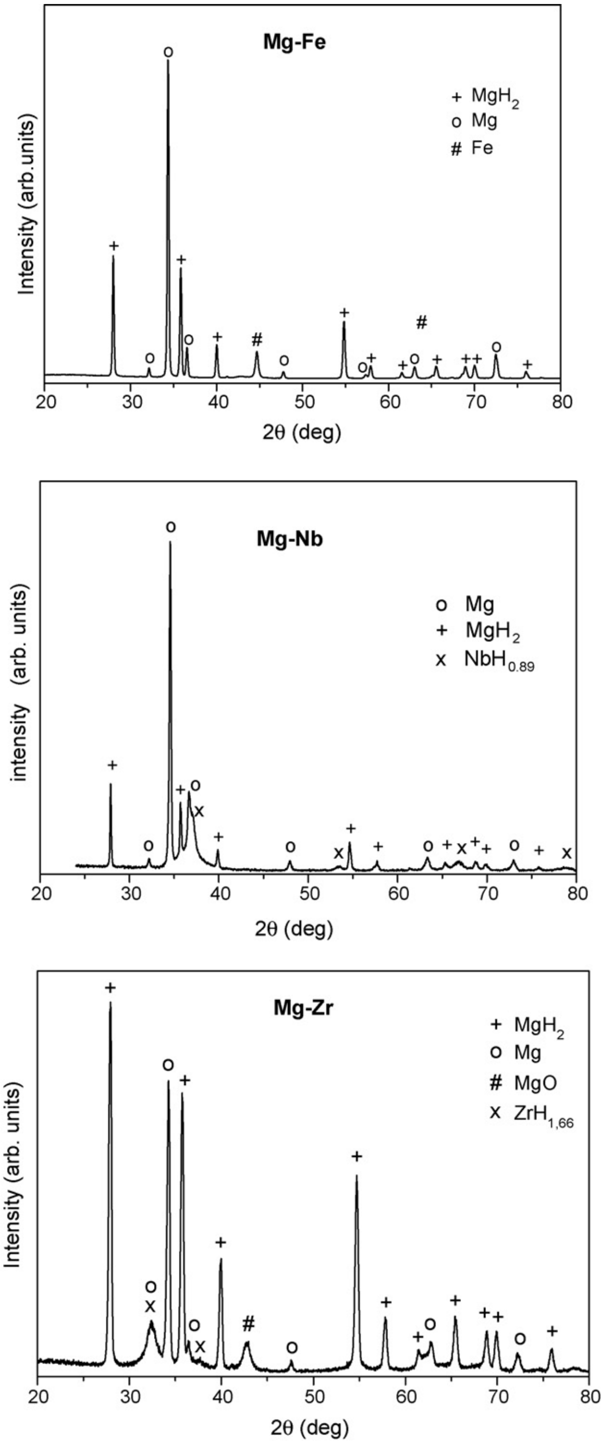

Fig. 1. Room temperature XRD spectra of the TM-doped MgH_2 samples, partially de-hydrogenated after their fully activation.

~3000 s for pure MgH_2 to ~100 s form Nb- and Fe-doped samples and ~200 s for the Zr-doped one.

In Fig. 3, we present the TDS spectra of the pure and TM-doped MgD_2 samples after their complete activation. The most important information provided by the spectra is the position of the peak temperature T_P at which the desorption rate reaches its maximum; this temperature allows a direct comparison of the influence of the TM additive on the thermal stability of the MgD_2 phase. The obtained spectra confirm the trend observed in the isothermal curves evidencing lower thermal stability of the TM-doped samples compared to pure MgD_2. The Fe- and Nb-doped samples show TDS peaks at ~470 and ~480 K, respectively, while the Zr-doped samples shows TDS peak at ~535 K. Pure MgD_2 shows the TDS peak at a larger temperature, close to 630 K.

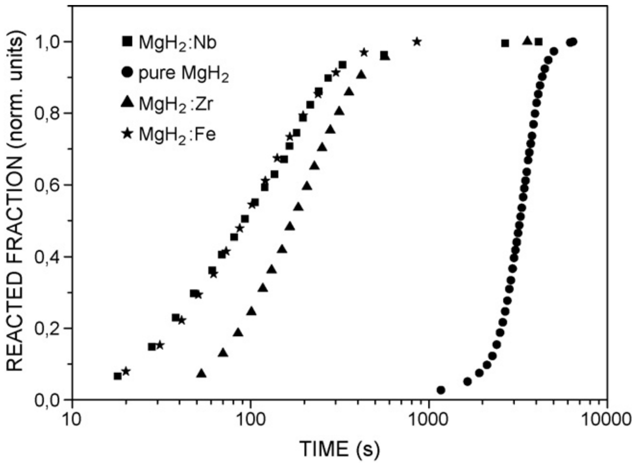

Fig. 2. Isothermal H_2 desorption curves of the pure and TM-doped MgH_2 samples at 623 K, after their fully activation.

Before going on with the discussion, it is important to remark that the Pd capping layer was deposited on the surface of all the prepared Mg films and consequently cannot explain the differences in the H_2 (or D_2) desorption kinetics of pure and TM-doped MgH_2 (or MgD_2) see Figs. 2 and 3.

The present H_2 (or D_2) desorption results show that the dispersion of different TM nanoclusters inside the MgH_2 matrix accelerate the H_2 desorption process. The catalytic process is thus connected with the acceleration of bulk processes, such as the nucleation and the growth of the h-Mg phase or the transport of H atoms to the Mg surface where their recombinative desorption occurs. The strong reduction of the nucleation time shown by the isothermal desorption curves of the TM-doped

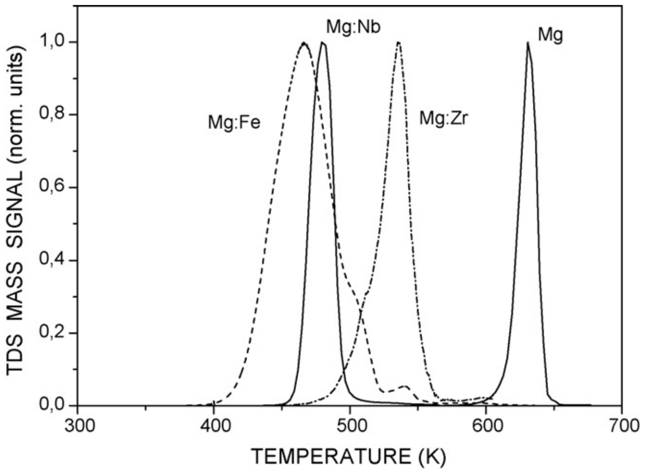

Fig. 3. TDS spectra of the pure and TM-doped MgD_2 samples after their fully activation.

samples (∼10 s for Nb and Fe, ∼50 s for Zr) compared to that pertinent to the pure MgD_2, ∼1000 s (see Fig. 3) suggests that the TM doping accelerates the nucleation process of the h-Mg phase. This indication is in line with previously published results on the isothermal H_2 desorption kinetics from Nb-doped MgH_2 samples indicating a change of the rate limiting step from the nucleation and growth of the h-Mg phase in pure MgH_2 to H atomic diffusion through interconnected h-Mg domains for Nb doping ranging between 2 and 5 at.% [15]. In solid-state reactions, such as the MgH_2 to h-Mg phase transition, new phases (h-Mg in the present H_2 desorption process) nucleate at extended defects of the parent one, such as grain boundaries, dislocations or interfaces with existing secondary phases. In the present samples the TM clusters dispersed in the MgH_2 matrix form extended MgH_2–TM interfaces. The efficiency of these interfaces in the h-Mg nucleation process is connected to the energetic features of the interface; an embryo of the h-Mg phase can reduce its energetic formation cost in MgH_2–TM interface as discussed, in general framework, in Ref. [16]. The important role of the interfaces in the catalysis of the hydrogen desorption process was indicated in a paper of Reule et al. [17] and von Zeppelin et al. [18]. The authors studied by TDS analysis the hydrogen desorption from MgH_2 powders catalysed by metallic additives; the maximum of the TDS peak was observed at 720 K for the pure MgH_2 while shifted to 500 K for MgH_2 catalysed by $La(Ni_{0.7}Fe_{0.3})_5$ and to 570 K for MgH_2 catalysed by $(Fe_{0.8}Mn_{0.2})Ti$. The microstructure of their samples, as studied by scanning electron microscopy (SEM), consisted on MgH_2 covering the additive particle like a film of irregular thickness. The authors attributed the improved desorption kinetics to the short diffusion path for H atoms inside MgH_2 layers and the large interface formed by MgH_2 and the metallic additive; the second point appeared as the most relevant because different additives may led to different catalytic effects. The MgH_2–TM interface can be a preferential nucleation site for the h-Mg phase also because of kinetic effects. In diffusional phase transitions where the transport of an atomic component occurs over paths longer that the interatomic distance, new phases are often observed to nucleate at grain boundaries of the parent phase; these extended defects result, in fact, fast diffusion channels for migrating atoms thus giving rise, in the lattice layers around them, to the critical solute concentration for the phase transition [19]. In the present TM-doped MgH_2 samples, the MgH_2–TM interface can play a similar role allowing an effective removal of the H atoms dissociated from adjacent MgH_2 layers and thus favouring the formation of h-Mg nuclei having critical size.

In the 400 to 700 K temperature range, where TDS peaks are observed, the equilibrium phase diagram of the Nb–H system indicates the formation of an interstitial solid solution of H in bcc Nb, the Zr–H phase diagram indicates the presence of both the stable hydride phase and the interstitial solid solution of H in hcp Zr, while Fe does not form any binary hydride phase and shows negligible H solubility. Figs. 2 and 3, thus, show that the TM nanoclusters catalyse the h-Mg phase nucleation even if they present different chemical affinity with hydrogen.

As indicated in the introduction, the rate limiting step in the hydrogen desorption from the Nb-doped MgH_2 samples (5 at.%) is given by the H atomic diffusion through h-Mg layers [8,9]; this mechanism was suggested by the evaluated value of the activation energy for desorption, 51 kJ/mol, close to that of the activation energy for H diffusion in h-Mg, 40 kJ/mol. Preliminary analyses indicate the same rate limiting step also in the Fe- and Zr-doped samples. This can be explained assuming that the h-Mg domains nucleated at the MgH_2–TM interfaces, grow and rapidly join together forming interconnected h-Mg domains where preferential diffusion of H atoms occurs. This mechanism is different from that occurring in pure microcrystalline MgH_2. Fernandez and Sanchez [20] suggested that the growth of the h-Mg nuclei was controlled by the hydrogen diffusion through β-MgH_2 layers and evaluated an activation energy value of about 100 kJ/mol for this process; the h-Mg phase nucleates in the bulk of MgH_2 (grain boundaries) and H atoms dissociated at the Mg–MgH_2 interface have to diffuse through the not reacted MgH_2 layers to reach the surface. In this case, the desorption paths give rise to a slower desorption kinetics as compared to that in TM-doped samples.

4. Conclusions

Composite materials consisting on TM-doped Mg (TM = Nb, Fe and Zr) with TM content in the 10^{-2} atomic concentration show reduced thermodynamic stability and accelerated H_2 desorption kinetics when compared to the pure MgH_2 samples. While in the pure MgH_2, the H_2 desorption kinetics is controlled by the nucleation and growth of the h-Mg phase with 141 kJ/mol activation energy, in TM-doped samples the H_2 release is controlled by the H diffusion through h-Mg layers with 51 kJ/mol activation energy. XRD analyses indicate the formation of TM nanoclusters in the hydride forming matrix; the improved H_2 desorption kinetics can be explained by the presence of extended interfaces between MgH_2 and TM nanoclusters acting as heterogeneous sites for the nucleation of the h-Mg phase and fast diffusion channels for H migrating atoms.

References

[1] R. Gonzalez, Y. Chen, K. Tang, Phys. Rev. B 26 (1982) 4637.

[2] S.A. Flodstoem, L.G. Petersson, S.B. Hagsstroem, J. Vac. Sci. Technol. 13 (1976) 280.

[3] G. Friedlmaier, M. Groll, J. Alloys Compd. 253-254 (1997) 550.

[4] A. Zaluska, L. Zaluski, J.O. Strom-Olsen, Appl. Phys. A72 (2001) 157.

[5] G. Liang, J. Huot, S. Boily, A. Van Neste, R. Schultz, J. Alloys Compd. 291 (1999) 295.

[6] J.F. Pelletier, J. Huot, M. Sutton, R. Schultz, A.R. Sandy, L.B. Lurio, S.G.J. Mochrie, Phys. Rev. B 63 (2001) 052103.

[7] A.R. Yavari, J.F.R. de Castro, G. Vaughan, G. Heunen, J. Alloys Compd. 353 (2003) 246.

[8] N. Bazzanella, R. Checchetto, A. Miotello, Appl. Phys. Lett. 85 (2004) 5212.

[9] R. Checchetto, N. Bazzanella, A. Miotello, P. Mengucci, J. Alloys Compd. 404–406 (2005) 461.

[10] R. Checchetto, N. Bazzanella, A. Miotello, C. Maurizio, F. D'Acapito, P. Mengucci, G. Barucca, G. Majini, Appl. Phys. Lett. 87 (2005) 061904.

[11] A.A. Nayeb-Hashemi, J.B. Clark (Eds.), Phase Diagrams of Binary Magnesium Alloys, ASM International, Materials Park, OH 44073, 1988.

[12] F.D. Manchester (Ed.), Phase Diagrams of Binary Hydrogen Alloys, ASM International, Materials Park, OH 44073, 2000.

[13] R. Checchetto, G. Trettel, A. Miotello, Meas. Sci. Technol. 15 (2004) 127.
[14] R. Checchetto, L.M. Gratton, A. Miotello, C. Cestari, Meas. Sci. Technol. 6 (1995) 1605.
[15] N. Bazzanella, R. Checchetto, A. Miotello, C. Sada, P. Mazzoldi, P. Mengucci, Appl. Phys. Lett. 89 (2006) 014101.
[16] D.A. Porter, K.E. Easterling, Phase Transformation in Metals and Alloys, Chapmann & Hall, London, 1992.
[17] H. Reule, M. Hirsher, A. Weisshardt, H. Kronmueller, J. Alloys Compd. 305 (2000) 246.
[18] F. von Zeppelin, H. Reule, M. Hirscher, J. Alloys Compd. 330–332 (2002) 723.
[19] D. Turnbull, in: F. Seitz, D. Turnbull (Eds.), Solid State Physics, vol. 3, Academic Press, New York, 1956.
[20] J.F. Fernandez, C.R. Sanchez, J. Alloys Compd. 340 (2002) 189.